IOPscience iopscience.iop.org

Home Search Collections Journals About Contact us My IOPscience

Magnetoresistance of magnetically doped ZnO films

This article has been downloaded from IOPscience. Please scroll down to see the full text article.

2009 J. Phys.: Condens. Matter 21 346001

(http://iopscience.iop.org/0953-8984/21/34/346001)

View the table of contents for this issue, or go to the journal homepage for more

Download details:
IP Address: 129.252.86.83
The article was downloaded on 29/05/2010 at 20:47

Please note that terms and conditions apply.

IOP PUBLISHING JOURNAL OF PHYSICS: CONDENSED MATTER

J. Phys.: Condens. Matter **21** (2009) 346001 (6pp) doi:10.1088/0953-8984/21/34/346001

Magnetoresistance of magnetically doped ZnO films

A J Behan[1], A Mokhtari[1], H J Blythe[1], M Ziese[2], A M Fox[1] and G A Gehring[1]

[1] Department of Physics and Astronomy, University of Sheffield, Sheffield S3 7RH, UK
[2] Division of Superconductivity and Magnetism, University of Leipzig, D-04103, Leipzig, Germany

E-mail: G.A.Gehring@sheffield.ac.uk

Received 1 December 2008, in final form 11 June 2009
Published 28 July 2009
Online at stacks.iop.org/JPhysCM/21/346001

Abstract

Magnetoresistance measurements have been made at 5 K on doped ZnO thin films grown by pulsed laser deposition. ZnCoO, ZnCoAlO and ZnMnAlO samples have been investigated and compared to similar films containing no transition metal dopants. It is found that the Co-doped samples with a high carrier concentration have a small negative magnetoresistance, irrespective of their magnetic moment. On decreasing the carrier concentration, a positive contribution to the magnetoresistance appears and a further negative contribution. This second, negative contribution, which occurs at very low carrier densities, correlates with the onset of ferromagnetism due to bound magnetic polarons suggesting that the negative magnetoresistance results from the destruction of polarons by a magnetic field. An investigation of the anisotropic magnetoresistance showed that the orientation of the applied magnetic field, relative to the sample, had a large effect. The results for the ZnMnAlO samples showed less consistent trends.

(Some figures in this article are in colour only in the electronic version)

1. Introduction

The search for spintronic materials that combine both semiconducting and ferromagnetic properties is currently one of the most active research fields in magnetism. Compounds based on ZnO are especially exciting in this context since, in contrast to GaMnAs and InMnAs, such thin films exhibit ferromagnetism at room temperature [1–7]. Despite the progress in developing ZnO as a spintronic material, there has been much controversy concerning the mechanism that causes the magnetism [8–11]. It has been found that not all doped films exhibit ferromagnetism and that the mobile carrier density, n_c, can be very different in those compounds that do [1, 9, 12–14].

The strong dependence of the magnetic response on the carrier density makes it interesting to investigate the magnetoresistance (MR). The MR gives the change in resistance with the applied magnetic field and hence probes the interaction between the itinerant carriers and the defect ions. In previous work, it has been found that the MR of transition metal (TM)-doped ZnO films can be positive, negative or a combination of the two due to competing mechanisms dominating in different fields [15]. This contrasts with undoped ZnO and ZnAlO samples, where the MR response is small, negative and temperature dependent [15–17]. The most commonly used TM dopant in ZnO is Co [15, 18–20]; thin films have also been studied when co-doped with Al [21, 22]. Films doped with Mn [19], as well as a combination of Mn and Co, have also been studied [23]. In this paper we investigate the MR of TM-doped ZnO samples both with and without Al co-doping. We first consider Co-doped samples, for which clear trends emerge, and then ZnMnAlO, for which the trends are less clear. Finally, we present results for anisotropic magnetoresistance (AMR) in Co-doped films.

2. Experimental details

Thin film, doped ZnO samples were grown by pulsed laser deposition (PLD) on *c*-cut sapphire substrates using a XeCl laser at 308 nm. Targets for ablation were prepared by grinding together appropriate amounts of high-purity MnO_2, Co_3O_4 and Al_3O_4 powders, pressing to pellet-form and then firing in air at various temperatures. The targets were then mounted in the deposition chamber on a rotating target-holder onto which

 © 2009 IOP Publishing Ltd Printed in the UK

Table 1. A summary of the data for the thin films shown in figures 1, 2 and 4. The labels given in column one identify the films and are marked on the figures. The second column gives the concentration of the dopants; the third column gives the oxygen pressure in the PLD chamber during film growth. The carrier density, n_c is quoted for 5 K. The final column is the saturation moment, M, in Bohr magnetons per TM ion, measured in the SQUID at 5 K.

Label	TM and Al concentration	O_2 (mTorr)	Thickness (nm)	n_c (cm^{-3}) at 5 K	M at 5 K
a, h	5% Co	10	30	2.0×10^{16}	1.38
b	5% Co	10	120	2.3×10^{18}	0.0
c	5% Co + 0.6% Al	5×10^{-2}	280	3.2×10^{19}	0.60
d, i	5% Co + 0.6% Al	5×10^{-2}	250	6.9×10^{20}	0.58
e	5% Co + 1.5% Al	5×10^{-2}	300	1.0×10^{21}	0.14
f	5% Co	10	80	1.2×10^{17}	0.0
g	5% Co	10	940	7.2×10^{18}	0.0
j	2% Mn + 0.5% Al	5×10^{-2}	520	1.2×10^{21}	0.50
k	2% Mn + 0.2% Al	5×10^{-2}	230	1.0×10^{21}	0.22
l	2% Mn + 0.8% Al	5×10^{-2}	290	1.6×10^{21}	0.38
m	2% Mn + 4.0% Al	6×10^{-2}	360	1.1×10^{21}	0.48
n	2% Mn + 1.2% Al	5×10^{-2}	850	1.6×10^{21}	0.0

the laser beam was focused. Substrates were mechanically clamped onto a heater, which could be swung into an optimum position with respect to the ablation plume. During deposition, the substrate temperature was held at 450 °C and the oxygen pressure could be varied between 10^{-2} and 100 mTorr. Film thickness, which could not be monitored directly during deposition, was determined, *inter alia*, by target–substrate separation; this was usually held at 35 mm. A film's thickness was controlled by varying the deposition time. Since the shape of the plume varied slightly both during a deposition, and also from deposition to deposition, and since the system did not have fixed geometry with respect to target and substrate positions, there was inevitably some slight variation of film thickness and characteristics between successive, isochronal depositions. A film's composition was assumed to be that of the respective target, although it is generally found that the dopant concentration in an ablated film is somewhat higher than in the target. It has been suggested [24, 25] that this arises due to the preferential sputtering of the host cation, in our case Zn, from the surface of the film over that of the dopant; this sputtering occurs due to the high-energy ions present in the incident laser plume; the effect was not investigated in the present work.

XRD patterns of typical targets and films have been made, when it was found that powder patterns indicated the targets to be single-phase with a hexagonal wurtzite structure. Traces of Al and Co metal, their respective oxides or any binary ZnCo phases were not observed in the target samples. Corresponding XRD patterns of the films indicate highly oriented growth; these results have been given earlier [14].

A wide range of samples was investigated with Co and Mn being the TM-dopants. Some of the Co-doped samples, and all of the Mn-doped samples, were also co-doped with Al. ZnO and ZnAlO samples with no TM-dopants were also studied for comparison. The Al co-doping was performed in order to generate a large, free-carrier density. It has also been established that free-carrier density varies with *intrinsic* defect concentration in the film; the latter was varied by depositing at various O_2 pressures; we have reported on this elsewhere [12].

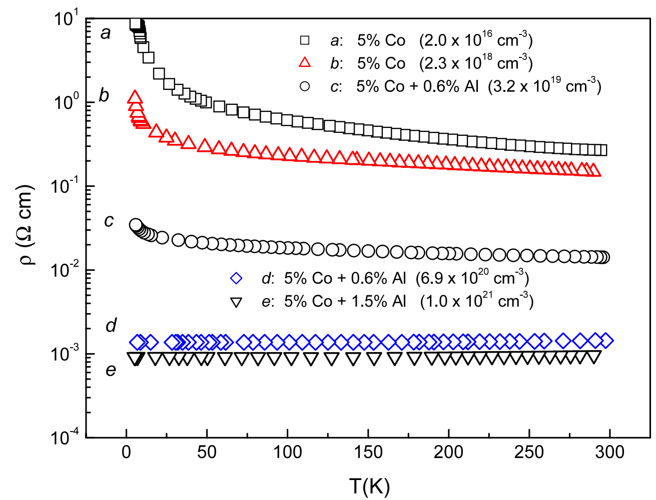

Figure 1. (Colour online) Resistivity, plotted on a logarithmic scale, as a function of temperature for 5% Co films containing different Al concentrations and grown at different deposition pressures and to different thicknesses; quoted carrier concentrations are for 5 K. Further detail is given in table 1.

Magnetization measurements were performed using a *Quantum Design* SQUID magnetometer; film thickness was measured with a *Dektak* profilometer. Carrier concentration and MR measurements were made using the van der Pauw four-probe method. The samples were mounted in a continuous-flow helium cryostat located between the pole pieces of an electromagnet; all measurements were made in reversible fields of up to 1 T. The MR is calculated from the expression, MR $= 100(\rho_B - \rho_0)/\rho_0$ where ρ_0 and ρ_B are the resistivities in zero and an applied field, B, respectively. All the measurements of MR reported here were made at 5 K, as the magnitude of the MR effect weakened as the temperature was raised. The anisotropy measurements were made by comparing the MR with the sample oriented perpendicular and parallel to the field for different current directions relative to that of the field direction. A summary of the results for the samples in figures 1, 2 and 4 is given in table 1.

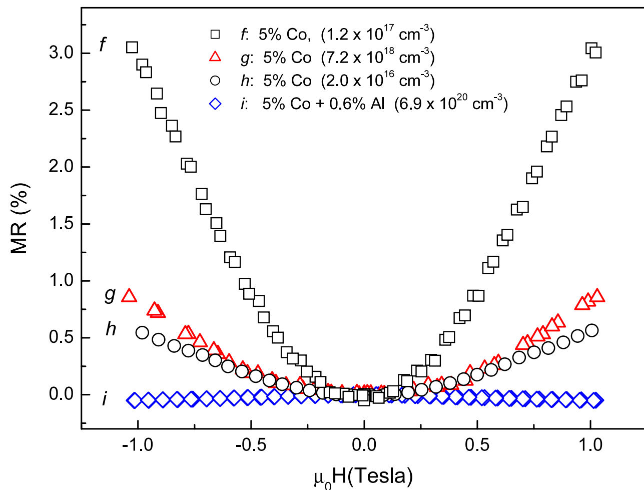

Figure 2. (Colour online) Magnetoresistance at 5 K as a function of field for ZnO films with 5% Co + varying amounts of Al; quoted carrier concentrations are for 5 K. Further detail is given in table 1.

2.1. Resistivity as a function of temperature

Before discussing the MR response, it is helpful to consider the temperature dependence of the resistivity in zero field. This allows us to classify the samples as metallic or insulating, and also to determine the carrier density. According to Matthiessen's rule, the electrical resistivity arises from the sum of electron scattering from defects and from phonons. The electron–phonon scattering is temperature dependent tending to zero as the temperature goes to zero, unlike defect scattering which is independent of temperature. Thus, even in a pure metal, the temperature dependence of the resistivity decreases to a finite value at zero temperature. This behaviour is in contrast to samples in which transport occurs via hopping between electron sites, with the hopping probability being proportional to the exponential of the difference in energy between the sites [26]. Since the energy gained to perform this hopping comes from lattice vibrations, the resistivity diverges at low temperatures, as the availability of phonons becomes less frequent [27].

In our samples, both metallic and hopping behaviour is observed. Figure 1 shows the temperature dependence of the resistivity of a series of 5% Co ZnO samples, some co-doped with Al ($Zn_{0.95-x}Co_{0.05}Al_xO$) with differing carrier concentrations and showing the transition from metallic to hopping conductivity; the resistivity is plotted on a logarithmic scale. The two films corresponding to labels a and b have different thicknesses but the same nominal compositions and were deposited under the same oxygen pressures. Despite this, the films have different carrier densities and give rise to different curves. However, in doped ZnO, film characteristics are notoriously sensitive to deposition conditions. The consequence of this is that, unless deposition parameters can be very tightly controlled, this invariably leads to some degree of irreproducibility in the film characteristics. Similar behaviour is also shown by films labelled c and d. Although we have not investigated this in any detail, we find generally that there is a variation in carrier concentration with film thickness. We attribute this, in part, to the decreasing level of strain in the thicker films, giving rise to different levels of intrinsic defects, which results in less traps for the carriers.

The samples with the highest carrier density show a resistivity typical of a 'dirty' metal: the resistivity tends to a constant value at low temperature and then increases with increasing temperature. As the carrier density decreases, the temperature dependence becomes what is expected for samples with localized carriers. The temperature dependence is that of variable range hopping at low temperatures, changing to thermally activated hopping as the temperature is raised; this has been reported in detail [12]. We thus find a change from metallic to hopping behaviour, which can be controlled by the Al content and, to a lesser extent, by the growth conditions, and this allows us to classify our samples' transport mechanisms.

3. Measurements of MR

3.1. Results for ZnO and ZnAlO films

In the absence of TM-dopants, all films show a small and negative MR caused by quantum corrections to the conductivity in the weak localization regime. Two electron waves may travel in opposite directions along the same closed path, being elastically scattered by the same impurities. This leads to a constructive interference and an additional resistance. Upon the application of a magnetic field, the two waves will acquire a phase difference so that the interference conditions are now violated and the additional resistance, present without the magnetic field, will decrease.

Films were grown with Al concentrations ranging between 0.2% and 1% and grown at the same oxygen pressure as the equivalent samples doped with Co. The Al-doped samples, with carrier concentrations of $\approx 10^{21}$ cm^{-3}, showed an MR value of around -0.2% in a field of 1 T. We note that, if each Al ion contributes one carrier, a doping of 1% of Al will give $n_c = 4.2 \times 10^{20}$ cm^{-3}. Hence only a small percentage of Al is required to take the film over the Mott limit of $\sim 3 \times 10^{19}$ cm^{-3}. However, for a pure ZnO sample with a much lower carrier concentration of 10^{18} cm^{-3}, the MR had a much larger value of -1.6%. This shows that the addition of Al reduces the effect causing the constructive interference. Since adding Al can increase disorder, it may be increasing the inelastic scattering [28]. Our results are in agreement with previous data on films grown by PLD [16] and sputtering [17].

3.2. Results for ZnCoO and ZnCoAlO films

When 5% Co is added to ZnO and ZnAlO, the MR curves can become very different. The data in figure 2 show the typical MR curves both with and without Al-doping. Most, but not all, samples of Al-doped ZnO are metallic for the reason discussed above and show a small and negative MR, independent of the Co content. However, samples without Al show hopping conductivity and can have positive MR, as observed for the $Zn_{0.95}Co_{0.05}O$ samples in figure 2.

Figure 3 shows the MR as a function of carrier density for a variety of ZnCoO and ZnCoAlO films. The magnetic moments of the films are indicated by the thickness of the data symbol. The general shapes of the MR curves are similar

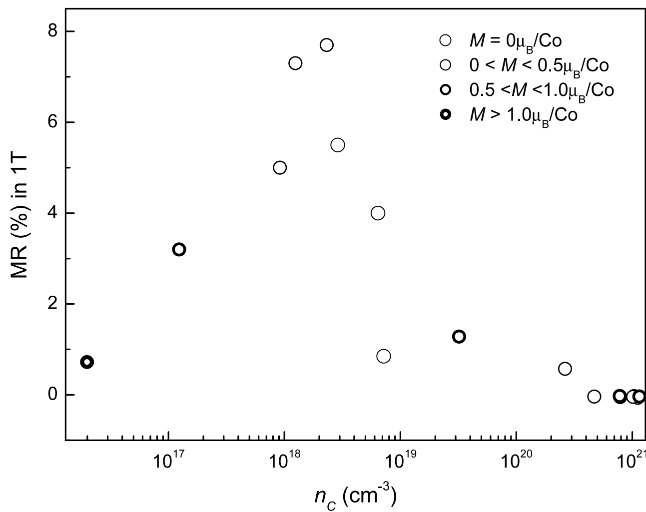

Figure 3. In-plane MR at 5 K as a function of carrier concentration for ZnO films doped with 5% Co and Al concentrations ranging from 0 to 1.5%. The magnitude of the moment, M, at 5 K is represented schematically by circles of increasing line-thickness.

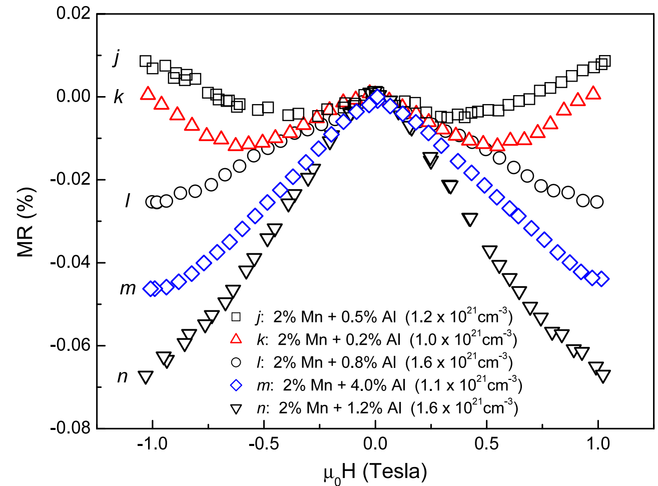

Figure 4. (Colour online) Magnetoresistance at 5 K as a function of field for ZnO films with 2% Mn + varying amounts of Al; quoted carrier concentrations are for 5 K; quoted carrier concentrations are for 5 K. Further detail is given in table 1.

to those shown in figure 2 but with magnitudes given by figure 3. We find that the MR becomes positive as the carrier concentration leaves the metallic regime, with the MR values measured at 1 T only becoming negative above 2×10^{20} cm^{-3}. The concentration for the Mott transition in our samples is estimated to be around 3×10^{19} cm^{-3}, which is similar to the value of 4.9×10^{19} cm^{-3} observed by Xu *et al* [29].

The positive MR can be attributed to electron redistribution from spin-splitting [29, 30] or by the increased polarization of the electrons that block the states for variable range hopping [31]. In the absence of a magnetic field, the resistivity arising from ionized impurity scattering will be dependent upon the relaxation time of the electrons at the Fermi level. This, in turn, will depend upon the position of the Fermi level and the impurity screening radius, r_0. As a field is applied and spin-splitting occurs, electron transfer will decrease the electron density of states at the Fermi level, leading to an increase in r_0. This implies a weaker Thomas–Fermi screening of the Coulomb potential, meaning an increase in electron localization as caused by Coulomb potential fluctuations. The relaxation times will increase, as will the resistivity, leading to a positive MR [30]. This effect is quenched as the electron density rises into the metallic regime because the Fermi energy is then larger than the spin-splitting energy.

It is most interesting to note that in figure 3 the magnitude of the MR begins to decrease again at carrier concentrations below 1×10^{18} cm^{-3}. This is most likely to be caused by the destruction of bound magnetic polarons (BMPs) by a decrease in disorder upon the application of the magnetic field. Evidence for this model comes from the fact that the magnetism increases as the MR at 1 T decreases. This agrees well with the theory where magnetism in insulating samples is attributed to the formation of BMPs [12]. The magnetic moment varies with carrier concentration. The zero magnetic moments fall in the region which, in Behan *et al* [12], we refer to as intermediate.

In figure 3 there is a strong correlation between carrier concentration and MR and any correlation between magnetic moment and MR is via carrier concentration. Hence two samples with different carrier concentrations, but similar MR values, can have very different magnetic moments.

3.3. Results for Mn-doped ZnAlO films

All the ZnMnO films for which we present results contain some Al. Films of ZnO doped only with Mn are so highly resistive that they are not reported here. The MR curves for Al-doped ZnO:Mn samples show a different MR behaviour to those considered previously. In several samples, the resistivity shows an initial decrease with field, followed by an increase at higher fields. The field at which the MR becomes positive varies from sample to sample, as shown in figure 4; this is in agreement with previous work [16]. The initial negative contribution is similar to that observed in Co-doped samples, although the positive contribution occurs at much higher carrier concentrations, including samples in the metallic regime. This obviously suggests that this positive contribution is much stronger in Mn- than in Co-doped samples. Attention is drawn to the change of scale between the Co and the Mn results, where the MR values for the films doped with Mn are all extremely small.

The MR at 1 T is plotted in figure 5 as a function of carrier concentration. In contrast to the results for the Co-doped samples, considerable scatter and no consistent trend is observed. A possible reason for the large scatter could be that the MR is known to be strongly temperature dependent [16], together with the small magnitude of the effect. Furthermore, since we are suggesting the positive and negative contributions come from screening and weak localization effects, respectively, we would not expect these to have magnetic dependencies.

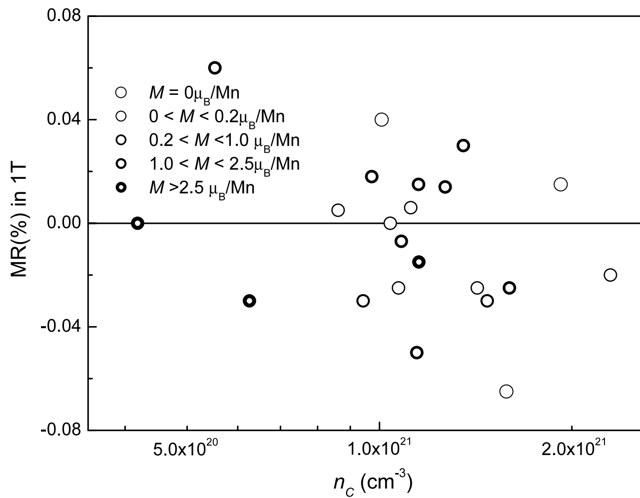

Figure 5. MR measured at 5 K in a parallel applied field of 1 T as a function of carrier concentration for ZnO films doped with 2% Mn and varying amounts of Al. The magnetic moments of the films, M, are represented by symbols of increasing line-width.

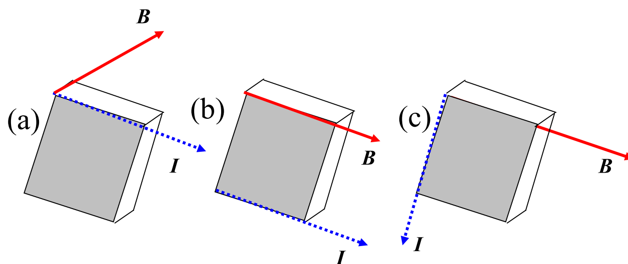

Figure 6. (Colour online) Various orientations of the magnetic field, B, and current, I, where the film's easy axis [001] lies in the shaded surface. Orientations (a), (b) and (c) will be referred to as perpendicular, longitudinal and transverse, respectively.

4. Measurements of AMR

AMR is only observed in magnetic materials and depends on the square of the spin–orbit coupling. In a thin film the current will be in-plane, whilst a magnetic field can be parallel or perpendicular to the film surface. There are therefore three useful geometries, as illustrated in figure 6.

Figure 7 presents MR results for films containing 5% Co and different concentrations of Al, in configurations (a)–(c), as described in figure 6. The results show that the MR is dependent upon the orientations of both the applied magnetic field and the current. All samples have thicknesses much larger than the mean free path and so any difference observed cannot be considered as a boundary effect. The results show consistently that, at carrier concentrations below 10^{20} cm^{-3}, the perpendicular MR for the configuration shown in figure 6(a) is much smaller than the MR when the magnetic field lies in the plane of the film, as in figures 6(b) and (c). There is a relatively small difference between the longitudinal MR, the configuration shown in figure 6(b), and the transverse MR, where the field lies in the plane but is perpendicular to the current. When considering the magnitude of the sample's

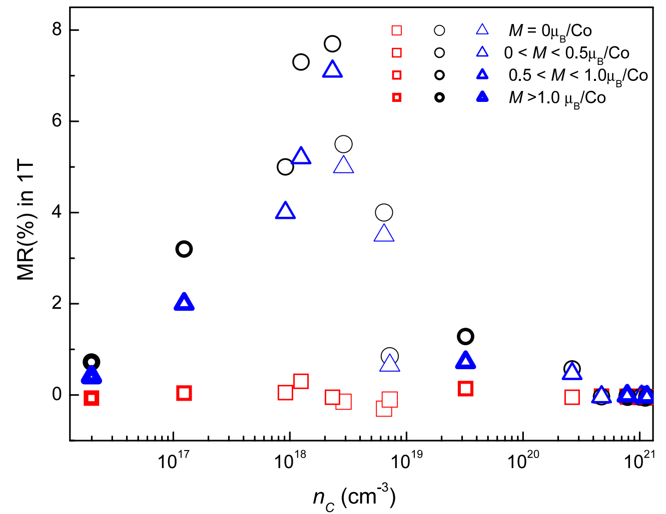

Figure 7. (Colour online) MR at 5 K and in a field of 1 T as a function of carrier concentration for ZnO films doped with 5% Co and varying amounts of Al in perpendicular (□), longitudinal (○) and transverse (△) orientations at 5 K. The magnitudes of the magnetic moments of the films at 5 K, M, are represented by symbols of increasing line-thickness.

magnetic moment compared to the difference in MR, we again see that a larger moment does not lead to a larger AMR. Indeed, the largest AMR is seen in samples which are not ferromagnetic. This leads us to the conclusion that the MR is strongly dependent upon current and field directions relative to the film. This MR dependency on film geometry has been observed in ZnCoO [32] and $SrRuO_3$ [33] thin films and a geometrical explanation has been proposed [34].

5. Conclusions

We have studied the variations of the MR response with carrier concentration in TM-doped ZnO thin films; carrier concentration has been varied by depositing the films at different oxygen pressures, to varying thicknesses and also by co-doping some samples with Al. Co-doped samples with high carrier concentrations show a small negative MR that is caused by weak localization effects; a decrease in the carrier concentration causes an increase in the positive MR contribution. This positive contribution originates from changes in Thomas–Fermi screening caused by a spin-splitting redistribution of electrons. At the lowest densities studied, another negative contribution is observed that correlates with the onset of ferromagnetism due to BMPs. This clearly suggests that the negative contribution is caused by the destruction of BMPs by a magnetic field. The MR response was found to be anisotropic with respect to the orientation of the magnetic field relative to the sample plane. The trends in the ZnMnAlO samples studied were less clear due to their much higher resistivities.

Acknowledgments

We should like to acknowledge EPSRC funding of this work through grants EP/D037581/1 and EP/D070406/1.

References

[1] Sharma P, Gupta A, Rao K V, Owens F J, Sharma R, Ahuja R, Osorio Guillen J M, Johansson B and Gehring G A 2003 *Nat. Mater.* **2** 673
[2] Venkatesan M, Fitzgerald C B, Lunney J G and Coey J M D 2004 *Phys. Rev. Lett.* **93** 177206
[3] Blythe H J, Ibrahim R M, Gehring G A, Neal J R and Fox A M 2004 *J. Magn. Magn. Mater.* **283** 117
[4] Özgür Ü, Alivov Ya I, Liu C, Teke A, Reshchikov M A, Doan S, Avrutin V, Cho S-J and Morkoç H 2005 *J. Appl. Phys.* **98** 041301
[5] Coey J M D, Venkatesan M and Fitzgerald C B 2005 *Nat. Mater.* **4** 173
[6] Norberg N S, Kittilstved K R, Amonette J E, Kukkadapu R K, Schwartz D A and Gamelin D R 2004 *J. Am. Chem. Soc.* **126** 9387
[7] Neal J R, Behan A J, Ibrahim R M, Blythe H J, Ziese M, Fox A M and Gehring G A 2006 *Phys. Rev. Lett.* **96** 197208
[8] Chambers S A 2006 *Surf. Sci. Rep.* **61** 345
[9] Coey J M D 2006 *Curr. Opin. Solid State Mater. Sci.* **10** 83
[10] Seshadri R 2005 *Curr. Opin. Solid State Mater. Sci.* **9** 1
[11] Kaspar T C, Droubay T, Heald S M, Nachimuthu P, Wang C M, Shutthandan V, Johnson C A, Gamelin D R and Chambers S A 2008 *New J. Phys.* **10** 055010
[12] Behan A J, Mokhtari A, Blythe H J, Score D S, Xu S H, Neal J R, Fox A M and Gehring G A 2008 *Phys. Rev. Lett.* **100** 047206
[13] Song C, Geng K W, Zeng F, Wang X B, Shen Y X, Pan F, Xie Y N, Liu T, Zhou H T and Fan Z 2006 *Phys. Rev.* B **73** 024405
[14] Xu X H, Blythe H J, Ziese M, Behan A J, Neal J R, Mokhtari A, Ibrahim R M, Fox A M and Gehring G A 2006 *New J. Phys.* **8** 135
[15] Gacic M, Jakob G, Herbort C and Adrian H 2007 *Phys. Rev.* B **75** 205206
[16] Andrearczyk T, Jaroszynski J, Grabecki G, Dietl T, Fukumura T and Kawasaki M 2005 *Phys. Rev.* B **72** 121309
[17] Liu X D and Jiang E Y 2007 *Solid State Commun.* **141** 394
[18] Fukumura T, Jin Z, Ohtomo A, Koinuma H and Kawasaki M 1999 *Appl. Phys. Lett.* **75** 3366
[19] Han S J, Song J W, Yang C H, Park S H, Park J H, Jeong Y H and Rhie K W 2002 *Appl. Phys. Lett.* **81** 4212
[20] Shlimak I, Khondaker S I, Pepper M and Ritchie D A 2000 *Phys. Rev.* B **61** 7253
[21] Kim J H, Kim H, Kim D, Ihm Y E and Choo W K 2003 *Physica* B **327** 304
[22] Hartmann L, Xu Q, Schmidt H, Hochmuth H, Lorenz M, Sturm C, Meinecke C and Grundmann M 2006 *J. Phys. D: Appl. Phys.* **39** 4920
[23] Wang J, Gui Z, Lu M, Wu D, Yuan C, Zhang S, Chen Y, Zhu S and Zhu Y 2006 *Appl. Phys. Lett.* **88** 252110
[24] van de Riet E, Kools J C S and Dielman J 1993 *J. Appl. Phys.* **73** 8290
[25] Dornless L S, O'Mahony D, Fitzgerald C B, McGee F, Venkatesan M, Stanca I, Lunney J G and Coey J M D 2005 *Appl. Surf. Sci.* **48** 406
[26] Mott N F 1990 *Metal Insulator Transitions* 2nd edn (London: Taylor and Francis)
[27] Ortuno M 1981 *J. Phys. C: Solid State Phys.* **14** 421
[28] Liu X J, Song C, Zeng F and Pan F 2007 *J. Phys.: Condens. Matter* **19** 296208
[29] Xu O, Hartmann L, Heidemarie-Schimdt H, Hochmuth A, Lorenz M, Schmidt-Grund R, Sturm C, Spemann D and Grundmann M 2006 *Phys. Rev.* B **73** 205342
[30] Shapira Y and Kautz R L 1974 *Phys. Rev.* B **10** 4781
[31] Yan S-S, Liu J P, Mei L M, Tian Y F, Song H Q, Chen Y X and Liu G L 2006 *J. Phys.: Condens. Matter* **18** 10469
[32] Lee J W, Kuroda S, Tanako F, Akinaga H and Takita K 2006 *Phys. Status Solidi* c **3** 4098
[33] Genish I, Kats Y, Klein L, Reiner J and Beasley M R 2004 *J. Appl. Phys.* **95** 6681
[34] Chaudhuri B K 2008 private communication